 CMES, vol.44, no.3, pp.249-279, 2009

An Optimal Fin Design Problem in Estimating the Shapes of Longitudinal and Spine Fully Wet Fins

Cheng-Hung Huang[1] **and Yun-Lung Chung**[1]

Abstract: The optimum shapes for the longitudinal and spine fully wet fins are estimated in the present inverse design problem by using the conjugate gradient method (CGM) based on the desired fin efficiency and fin volume. One of the advantages in using CGM in the inverse design problem lies in that it can handle problems having a large number of unknown parameters easily and converges very fast. Results obtained by using the CGM to solve the inverse design problems are justified based on the numerical experiments. Results show that when the Biot number and relative humidity are varied, the optimum fin efficiency and optimum fin shape will also be changed.

Nomenclature

$\bar{A}(\bar{x})$	cross-section area of fin
Bi_1, Bi_2	Biot number
$\bar{h}_1, \bar{h}_2$	convective heat transfer coefficient
$\bar{h}_m$	mass transfer coefficient
$\bar{h}_{fg}$	latent heat of condensation of moisture
J	functional defined by equation (3)
J'	gradient of functional defined by equation (17)
$\bar{k}$	thermal conductivity
$\bar{L}$	reference length
$\bar{p}(\bar{x})$	perimeter of fin
q	actual heat transfer rate through fin
Q	ideal heat transfer rate through fin
$r(x)$	fin radius for spine fins and fin thickness for longitudinal fins
$\bar{T}$	dimensional temperature of fin
$v(r)$	estimated fin volume
V	given fin volume

[1] Department of Systems and Naval Mechatronic Engineering, National Cheng Kung University, Tainan, Taiwan 701, R.O.C. Email: e-mail: chhuang@mail.ncku.edu.tw

w fin width

Greeks

α weighting coefficient
β search step size
γ conjugate coefficient
$\theta(x)$ estimated dimensionless temperature of fin
$\Delta\theta(x)$ sensitivity function defined by equation (8)
Ω computational domain
$\lambda(x)$ Lagrange multiplier defined by equation (15)
$\delta(\cdot)$ Dirac delta function
η estimated fin efficiency
Φ desired fin efficiency
ε convergence criteria
$\bar{\omega}$ specific humidity
$\bar{\omega}_a$ specific humidity of surrounding air

Superscript

n iteration index
$\_$ dimensional quantities

1 Introduction

Finned surfaces have been in use over a long period of time for dissipation of heat by convection or by radiation. Finned surfaces are widely seen in many engineering applications such as air-conditioning, refrigeration, cryogenics and cooling systems in industrial. For this reason it is quite nature that many works have been done in order to improve the design of the fins.

The design criterions of fins are different for various applications, but the primary concern is the fin volume (or weight) and fin efficiency and it is highly desirable to optimize the shape of fins based on these two constraints. The optimum dimensions are those for which maximum (or desired) fin efficiency is obtained for some fixed volume of the fin. Although the fin efficiency of the estimated fin by optimum design process is superior than that for the conventional fin, it may be limited to use in actual practice since the resulting profile shape may be difficult to manufacture and fabricate.

Numerous studies have been conducted to optimize the dimensions of spine and longitudinal fins of various profiles subject to convection. For pure conducting fins, a criterion for optimum shape was proposed by Schmidt (1926) using the principle of a constant heat flux. This result was confirmed later by Duffin (1959) by using a variational method. In their studies, the fin profile is calculated as a parabola and has a zero thickness at the outer edge. An optimum shape of purely radiating fin was obtained by Wilkins (1960) for a variety of geometries. For convective and radiative fins, Kern and Kraus (1972) have presented a thorough study of the optimum design of finned surfaces. Aziz (1992) has published a survey article where the optimum dimensions of straight fins, annular fins and spines of different profiles with many numerical examples are included. Razelos (1983) and Chung (1983) have independently presented the optimum dimensions of convective pin fin with cylindrical, conical, concave parabolic and convex parabolic profiles. A review on extended surfaces over six decades is available in the work by Kraus (1988). Chung and Iyer (1993) used an integral approach to determine the optimum dimensions for rectangular longitudinal fins and cylindrical pin fins. Yeh (1996) used the Lagrange's multiplier method to find the optimum dimensions of longitudinal rectangular and cylindrical pin fins.

In all the references above the optimum shape of fins are determined based on either minimum weight or maximum heat transfer rate through fin base. The fin design problems based on desired fin efficiency for some specified fin volume have never been seen in the literatures. For this reason, Huang and Hsiao (2003) and Huang and Wu (2007) developed the inverse design algorithm using Conjugate Gradient Method (CGM) to estimate the optimum shapes for Fourier and Non-Fourier fins, respectively, based on desired fin efficiency.

For the air conditioning equipment, the surface temperature of the evaporator fin is generally below the dew point of the surrounding air and therefore moisture is condensed on the fin surface to evolve latent heat. For this reason mass transfer occurs simultaneously with the heat transfer. Many investigations [McQuiston (1975), Coney, Sheppard and El-Shafei (1989), Wu and Bong (1994), Kundu (2002, 2007) and Pirompugd, Wang and Wongwises (2007)] have devoted to analyze the effect of condensation on the performance of different fins for only some fixed geometry, i.e. the direct problem analysis.

Recently Kundu (2008) applied the variational principle to determine the optimum profiles of longitudinal, annular and spine fins, respectively, operating in dehumidifying conditions. The cost function is selected as the maximization of heat transfer rate and the design constraints are selected as either fin volume or both fin volume and length. Sharqawy and Zubair (2008) examined the closed-form solutions for efficiency of fully wet straight fins of different configurations when subjected to

simultaneous heat and mass transfer mechanisms. For any given fin profile area they will find the optimum fin thickness by keeping all parameters constant and considering fin thickness as the only independent variable in the fin heat transfer equation. The cost function is also selected as the maximization of heat transfer rate.

Various inverse algorithms have been applied to many different engineering practical applications. Huang and Chen (2008) applied the steepest descent method (SDM) in a three-dimensional shape identification problem to estimate the unknown irregular shape of internal cavity. Jeong and Kallivokas (2008) employed the apparatus of partial-differential-equation-constrained optimization to the inverse scattering problem in identifying the shape and location of a rigid scatterer fully buried in a homogeneous halfplane, when illuminated by surficial (line) wave sources generating SH waves. Liu (2008) applied a Lie-group shooting method to the inverse vibration problem to simultaneously estimate the time-dependent damping and stiffness functions by using two sets of displacement as inputs. Mera et al (2006) developed an inverse algorithm by combining evolution strategies, the boundary element method and super-elliptical parameterization for detecting inclusions parameterized by super ellipses in non-destructive evaluation and testing.

The objective of the present work is to develop an inverse design algorithm using the Conjugate Gradient Method (CGM) to estimate the optimum shapes of the spine and longitudinal wet fins based on desired fin efficiency. This subject has never been examined before.

In this work the algorithm of the CGM in estimating the optimum shapes of spine and longitudinal wet fins based on desired fin efficiency for some specified fin volume will be given in detail. Moreover, the influence of relative humidity and Biot number on the optimum fin shape is also discussed. The CGM derives from perturbation principle, and transforms the inverse problem to the solution of three problems, namely, the direct problem, the sensitivity problem and the adjoint problem. The above three problems will be derived in the next few sections.

2 The Direct Problem

The following fin design problem is considered to illustrate the methodology in designing the optimum shape for the spine and longitudinal fully wet fins based on the desired fin efficiency and a specified fin volume.

The mathematical expression for the steady-state fully wet fin problem in dimensional form can be obtained as:

$$\frac{d}{d\bar{x}}[\bar{A}(\bar{x})\frac{d\bar{T}}{d\bar{x}}] = \frac{\bar{h}_1\bar{p}(\bar{x})}{\bar{k}}\{\bar{T}-\bar{T}_a+\bar{h}_{fg}\frac{\bar{h}_m}{\bar{h}_1}[\bar{\omega}(\bar{T})-\bar{\omega}_a]\};\ \text{in } 0<\bar{x}<\bar{L} \text{ in } \Omega \qquad (1a)$$

$$\bar{T} = \bar{T}_b;\ \text{at}\ \bar{x} = 0 \tag{1b}$$

$$\bar{k}\frac{d\bar{T}}{d\bar{x}} + \bar{h}_2\bar{T} = \bar{h}_2\bar{T}_a;\ \text{at}\ \bar{x} = \bar{L} \tag{1c}$$

here the over-bar "‾" represents dimensional quantities.

$\bar{A}(\bar{x})$ and $\bar{p}(\bar{x})$ represent the cross-section area and perimeter of fin; $\bar{k}$ is the constant thermal conductivity of fin; $\bar{T}_b$ and $\bar{T}_a$ are the fin base temperature at $\bar{x} = 0$ and ambient air temperature, respectively. $\bar{h}_1$ and $\bar{h}_2$ are the heat transfer coefficients on fin surface and at fin tip $\bar{x} = \bar{L}$, respectively. $\bar{h}_m$ and $\bar{h}_{fg}$ are the mass transfer coefficient and latent heat of condensation of moisture, respectively, $\bar{\omega}$ and $\bar{\omega}_a$ represent the specific humidity and specific humidity of surrounding air, respectively.

For spine fins $\bar{A}(\bar{x}) = \pi\bar{r}(\bar{x})^2$ and $\bar{p}(\bar{x}) = 2\pi\bar{r}(\bar{x})$, and $\bar{r}(\bar{x})$ represents fin radius. For longitudinal fins $\bar{A}(\bar{x}) = \bar{r}(\bar{x}) \times \bar{w}$ and $\bar{p}(\bar{x}) \approx 2\bar{w}$, (the assumption of $\bar{r}(\bar{x}) \ll \bar{w}$ is used) and $\bar{r}(\bar{x})$ is fin thickness. Here $\bar{w}$ is the width of longitudinal fins.

If the following dimensionless quantities are defined

$$\theta = \frac{\bar{T}_a - \bar{T}}{\bar{T}_a - \bar{T}_b};\quad x = \frac{\bar{x}}{\bar{L}};\quad r = \frac{\bar{r}}{\bar{L}};\quad Bi_1 = \frac{\bar{h}_1\bar{L}}{\bar{k}};\quad Bi_2 = \frac{\bar{h}_2\bar{L}}{\bar{k}};\quad w = \frac{\bar{w}}{\bar{L}}$$

Finally the dimensionless fully wet fin equation can be obtained as

$$\frac{d}{dx}\left[F_1(x)\frac{d\theta(x)}{dx}\right] = 2Bi_1F_2(x)\{\theta(x) + \bar{h}_{fg}\frac{\bar{h}_m}{\bar{h}_1}\frac{[\omega(\bar{T}) - \bar{\omega}_a]}{(\bar{T}_b - \bar{T}_a)}\ ;\ \text{in}\ 0 < x < 1 \tag{2a}$$

$$\theta = 1;\ \text{at}\ x = 0 \tag{2b}$$

$$\frac{d\theta}{dx} + Bi_2\theta = 0;\ \text{at}\ x = 1 \tag{2c}$$

Where $F_1(x) = r(x)^2$ and $F_2(x) = r(x)$ for spine fully wet fins while $F_1(x) = r(x)$ and $F_2(x) = 1.0$ for longitudinal fully wet fins. Besides, in accordance with the Chilton-Colburn analogy [Threlkeld (1970)], we have $\frac{\bar{h}_1}{\bar{h}_m} = C_{\text{p,a}}L_e^{2/3}$. Figures 1a and 1b illustrate the dimensionless geometry for the longitudinal and spine fully wet fins considered here.

The direct problem considered here is concerned with the determination of the temperature distribution of fully wet fin and its efficiency when the shape of fin and the boundary conditions are given and known.

3 The Fully Wet Fin Design Problem

For the fully wet fin design problem, the shape of fully wet fin, i.e. r(x), is regarded as being unknown, but everything else in equation (2) is known. In addition, the desired fin efficiency and fin volume are specified.

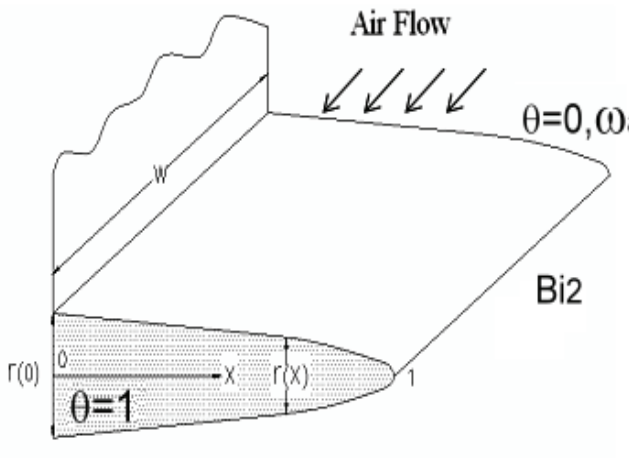

Figure 1(a): The longitudinal fully wet fin.

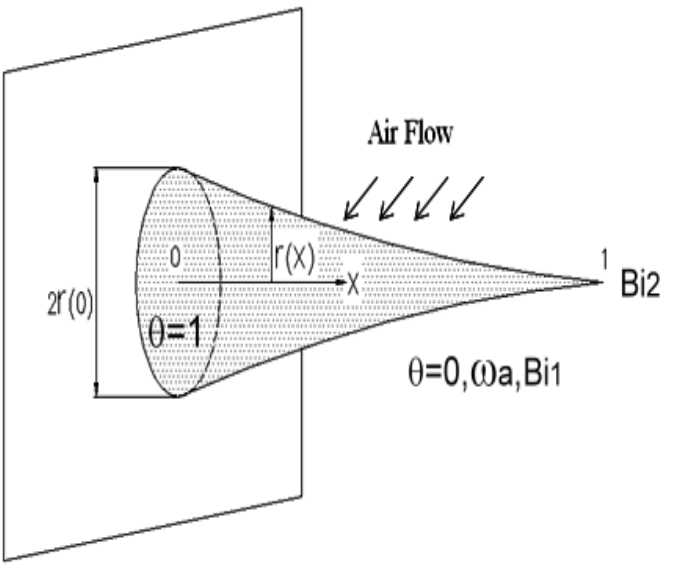

Figure 1(b): The spine fully wet fin.

The solution of the present fin design problem is to be obtained in such a way that the following functional is minimized:

$$J(r) = [q(r) - \Phi Q(r)]^2 + \alpha[v(r) - V]^2 \tag{3}$$

here q(r) and Q(r) are the actual (or estimated) and ideal heat transfer rate of fully wet fin, respectively. v(r) and V represent the estimated and desired (or given) fin volume. Φ is the desired fin efficiency and α is the weighting coefficient.

The first term on the right hand side is the square of the deviation between the actual and desired heat transfer rate through fully wet fin. The second term on the right hand side is the square of the deviation between the estimated and desired fin volume.

If the value of functional J(r) is less than the specified stopping criterion ε, stop the iterative process and the optimal shape of fully wet fins is obtained, otherwise, continue the iteration until the stopping criterion is satisfied.

Here $q = \frac{\bar{q}}{\bar{q}_{ref}}$, $Q = \frac{\bar{Q}}{\bar{q}_{ref}}$ and $v = \frac{\bar{v}}{\bar{v}_{ref}}$ are defined and the reference quantities and are given as

$$\bar{q}_{ref} = \bar{h}_1 \bar{L}^2 (\bar{T}_a - \bar{T}_b) \tag{4a}$$

$$\bar{v}_{ref} = \bar{L}^3 \tag{4b}$$

For spine fins we have

$$\bar{q} = \int_{\bar{x}=0}^{\bar{L}} \bar{h}_1 [2\pi \bar{r}(\bar{x})] \{(\bar{T}_a - \bar{T}) + \bar{h}_{fg} \frac{\bar{h}_m}{\bar{h}_1} [\bar{\omega}_a - \omega(\bar{T})]\} d\bar{x} \tag{5a}$$

$$\bar{Q} = \int_{\bar{x}=0}^{\bar{L}} \bar{h}_1 [2\pi \bar{r}(\bar{x})] \{(\bar{T}_a - \bar{T}_b) + \bar{h}_{fg} \frac{\bar{h}_m}{\bar{h}_1} [\bar{\omega}_a - \bar{\omega}_b]\} d\bar{x} \tag{5b}$$

$$\bar{v} = \int_{\bar{x}=0}^{\bar{L}} \pi \bar{r}(\bar{x})^2 d\bar{x} \tag{5c}$$

therefore the dimensionless quantities for q, Q and v can be obtained as

$$q = \int_{x=0}^{1} 2\pi r(x) \{\theta(x) + \bar{h}_{fg} \frac{\bar{h}_m}{\bar{h}_1} \frac{[\bar{\omega}_a - \omega(\bar{T})]}{(\bar{T}_a - \bar{T}_b)}\} dx \tag{5d}$$

$$Q = \int_{x=0}^{1} 2\pi r(x)\{1 + \bar{h}_{fg}\frac{\bar{h}_m}{\bar{h}_1}\frac{[\bar{\omega}_a - \bar{\omega}_b]}{(\bar{T}_a - \bar{T}_b)}\}dx \tag{5e}$$

$$v = \int_{x=0}^{1} \pi r(x)^2 dx \tag{5f}$$

For longitudinal fins, we assumed $\bar{r}(\bar{x}) \ll \bar{w}$ to obtain

$$\bar{q} = \int_{\bar{x}=0}^{\bar{L}} \bar{h}_1(2\bar{w})\{(\bar{T}_a - \bar{T}) + \bar{h}_{fg}\frac{\bar{h}_m}{\bar{h}_1}[\bar{\omega}_a - \omega(\bar{T})]\}d\bar{x} \tag{6a}$$

$$\bar{Q} = \int_{\bar{x}=0}^{\bar{L}} \bar{h}_1(2\bar{w})\{(\bar{T}_a - \bar{T}_b) + \bar{h}_{fg}\frac{\bar{h}_m}{\bar{h}_1}[\bar{\omega}_a - \bar{\omega}_b]\}d\bar{x} \tag{6b}$$

$$\bar{v} = \int_{\bar{x}=0}^{\bar{L}} \bar{w}\bar{r}(\bar{x})d\bar{x} \tag{6c}$$

Finally the dimensionless quantities for q, Q and v can be expressed as

$$q = \int_{x=0}^{1} 2w\{\theta(x) + \bar{h}_{fg}\frac{\bar{h}_m}{\bar{h}_1}\frac{[\bar{\omega}_a - \omega(\bar{T})]}{(\bar{T}_a - \bar{T}_b)}\}dx \tag{6d}$$

$$Q = \int_{x=0}^{1} 2w\{1 + \bar{h}_{fg}\frac{\bar{h}_m}{\bar{h}_1}\frac{[\bar{\omega}_a - \bar{\omega}_b]}{(\bar{T}_a - \bar{T}_b)}\}dx \tag{6e}$$

$$v = \int_{x=0}^{1} wr(x)dx \tag{6f}$$

The fully wet fin design problem can now be stated as follows: by utilizing the above mentioned functional J[r(x)], estimate the optimum shape of fully wet fin, i.e. the values of r(x), such that the actual (or estimated) heat transfer rate of fully wet fin, q, approaches to ΦQ and the estimated fin volume, v, approaches to the desired fin volume, V.

The conjugate gradient method has the ability in optimizing the above fin design problem and will be discussed in detail in the next section.

4 Conjugate Gradient Method (CGM) for Minimization

The following iterative process based on the CGM [Alifanov (1974)] is now used to estimate the unknown fin shape r(x) by minimizing the functional $J[r(x)]$.

$$r^{n+1}(x) = r^n(x) - \beta^n P^n(x) \tag{7a}$$

Here β^n is the search step size in going from iteration n to iteration n+1 and $P^n(x)$ is the direction of descent (i.e. search direction) given by

$$P^n(x) = J'^n(x) + \gamma^n P^{n-1}(x) \tag{7b}$$

which is a conjugation of the gradient in the outward normal direction $J'^n(x)$ at iteration n and the direction of descent $P^{n-1}(x)$ at iteration n-1. The conjugate coefficient is defined as [Alifanov (1974)]

$$\gamma^n = \int_{x=0}^{1} (J'^n)^2 dx \Big/ \int_{x=0}^{1} (J'^{n-1})^2 dx; \quad \text{with } \gamma 0 = 0 \tag{7c}$$

It should be noted that when $\gamma^n = 0$ for any n, in equation (7b), the direction of descent $P^n(x)$ becomes the gradient direction, i.e. the Steepest Descent Method (SDM) is obtained. The convergence of the above iterative procedure in minimizing the functional J is guaranteed in [Lasdon, Mitter and Warren (1967)].

To perform the iterations according to equation (7a), we need to compute a search step size β^n and the gradient of the functional $J'^n(x)$. In order to develop expressions for the determination of these two quantities, a "sensitivity problem" and an "adjoint problem" need be constructed as described below.

5 Sensitivity Problem and Search Step Size

The sensitivity problem can be obtained from the original direct problem defined by equation (2) in the following manner: It is assumed that when r(x) undergoes a variation $\Delta r(x)$, $\theta(x)$ and $\bar{\omega}$ are perturbed by $\Delta\theta(x)$ and $\Delta\bar{\omega}$, respectively. Replacing in the direct problem $r(x)$ by $r(x)+\Delta r(x)$, $\theta(x)$ by $\theta(x)+\Delta\theta(x)$ and $\bar{\omega}$ by $\bar{\omega}+\Delta\bar{\omega}$, subtracting the resulting expressions from the direct problem and neglecting the second-order terms, the following sensitivity problem for the sensitivity function $\Delta\theta(x)$ are obtained.

$$\frac{d}{dx}[F_3(x)\frac{d\Delta\theta}{dx}] + \frac{d}{dx}[F_4(x)\frac{d\theta}{dx}] = 2Bi_1 F_5(x) + 2Bi_1 \frac{\bar{h}_m \bar{h}_{fg}}{(\bar{T}_b - \bar{T}_a)\bar{h}_1} F_6(x); \text{ in } 0 < x < 1 \tag{8a}$$

$$\Delta\theta = 0;\ \text{at } x = 0 \tag{8b}$$

$$\frac{d\Delta\theta}{dx} + Bi_2\Delta\theta = 0;\ \text{at } x = 1 \tag{8c}$$

here $F_3(x) = r(x)^2, F_4(x) = 2r(x)\Delta r(x)$, $F_5(x) = r(x)\Delta\theta(x) + \theta(x)\Delta r(x)$ and $F_6(x) = r(x)\Delta\bar{\omega} + \bar{\omega}\Delta r(x) - \bar{\omega}_a\Delta r(x)$ for spine fins while $F_3(x) = r(x)$, $F_4(x) = \Delta r(x)$, $F_5(x) = \Delta\theta(x)$ and $F_6(x) = \Delta\bar{\omega}$ for longitudinal fins.

The functional $J(r^{n+1})$ for iteration $n+1$ is obtained by rewriting equation (3) as

$$J(r^{n+1}) = [q(r^n - \beta^n p^n) - \Phi Q(r^n - \beta^n p^n)]^2 + \alpha[v(r^n - \beta^n p^n) - V]^2 \tag{9a}$$

where we have replaced r^{n+1} by the expression given by equation (7a). If the terms $q(r^n - \beta^n p^n)$, $Q(r^n - \beta^n p^n)$ and $v(r^n - \beta^n p^n)$ are linearized by a Taylor expansion, equation (9a) takes the form

$$J(r^{n+1}) = \{q(r^n) - \beta^n[\Delta q(p^n) - \Phi\Delta Q(p^n)] - \Phi Q(r^n)\}^2 + \alpha[v(r^n) - \beta^n\Delta v(p^n) - V]^2 \tag{9b}$$

Here the expressions for Δq, ΔQ and Δv can be obtained by using $\Delta q = q(r+\Delta r) - q(r)$, $\Delta Q = Q(r+\Delta r) - Q(r)$ and $\Delta v = v(r+\Delta r) - v(r)$ and neglecting the high order terms. Eventually, for spine fully wet fins we have

$$\Delta q = \int_{x=0}^{1} 2\pi\{r\Delta\theta + \theta\Delta r + \bar{h}_{fg}\frac{\bar{h}_m}{\bar{h}_1}\frac{[\Delta r(\bar{\omega}_a - \bar{\omega}(\bar{T})) - r\Delta\bar{\omega}(\bar{T})]}{(\bar{T}_a - \bar{T}_b)}\}dx \tag{10a}$$

$$\Delta Q = \int_{x=0}^{1} 2\pi\Delta r\left[1 + \bar{h}_{fg}\frac{\bar{h}_m}{\bar{h}_1}\frac{(\bar{\omega}_a - \bar{\omega}_b)}{(\bar{T}_a - \bar{T}_b)}\right]dx \tag{10b}$$

$$\Delta v = \int_{x=0}^{1} 2\pi r\Delta r dx \tag{10c}$$

for longitudinal fully wet fins we have

$$\Delta q = \int_{x=0}^{1} 2w\{\Delta\theta - \bar{h}_{fg}\frac{\bar{h}_m}{\bar{h}_1}\frac{[\Delta\omega(\bar{T})]}{(\bar{T}_a - \bar{T}_b)}\}dx \tag{11a}$$

$$\Delta Q = 0 \tag{11b}$$

$$\Delta v = \int_{x=0}^{1} w\Delta r dx \tag{11c}$$

The sensitivity function $\Delta\theta(x)$ is taken as the solutions of problem (8) by letting $\Delta k = -P^n$. Once $\Delta\theta$(x) is obtained, the above quantities can all be calculated.

The search step size β^n is determined by minimizing the functional given by equation (9b) with respect to β^n. The following expression results:

$$\beta^n = \frac{(q-\Phi Q)(\Delta q - \Phi \Delta Q) + \alpha (v-V)\Delta v}{(\Delta q - \Phi \Delta Q)^2 + \alpha \Delta v^2} \tag{12}$$

6 Adjoint Problem and Gradient Equation

To obtain the adjoint problem, equation (2a) is multiplied by the Lagrange multiplier (or adjoint function) $\lambda(x)$ and the resulting expression is integrated over the correspondent space domain. The result is then added to the right hand side of equation (3) to yield the following expression for the functional $J[r(x)]$:

$$J(r) = (q-\Phi Q)^2 + \alpha (v-V)^2 + \int_{x=0}^{1} \lambda(x)\{\frac{d}{dx}[F_1(x)\frac{d\theta(x)}{dx}] - 2Bi_1 F_2(x)\{\theta(x) + \bar{h}_m \bar{h}_{fg} \frac{[\bar{\omega}(\bar{T}) - \bar{\omega}_a]}{(\bar{T}_b - \bar{T}_a)\bar{h}_1}\} dx \tag{13}$$

The variation ΔJ is obtained by perturbing r by $r+\Delta r$, θ by $\theta + \Delta\theta$, q by $q + \Delta q$, Q by $Q + \Delta Q$ and v by $v + \Delta v$ in equation (13), subtracting from the resulting expression the original equation (13) and neglecting the second-order terms. We thus find

$$\Delta J = 2(q-\Phi Q)(\Delta q - \Phi \Delta Q) + \alpha[2(v-V)\Delta v] + \int_{x=0}^{1} \lambda(x)\{\frac{d}{dx}[F_3(x)\frac{d\Delta\theta}{dx}] + \frac{d}{dx}[F_4(x)\frac{d\theta}{dx}] - 2Bi_1 F_5(x) - 2Bi_1 \frac{\bar{h}_m \bar{h}_{fg}}{(\bar{T}_b - \bar{T}_a)\bar{h}_1} F_6(x)\} dx \tag{14}$$

In equation (14), the domain integral term is reformulated using integration by parts; the boundary conditions of the sensitivity problem given by equations (8b) and (8c) are utilized and then ΔJ is allowed to go to zero. The vanishing of the integrands containing $\Delta\theta$ leads to the following adjoint problem for the determination of $\lambda(x)$:

$$\frac{d}{dx}[F_7(x)\frac{d\lambda}{dx}] + 4(q-\Phi Q)F_8(x) = 2\lambda Bi_1 F_9(x)[1 + \frac{d\bar{\omega}}{d\theta}\frac{\bar{h}_m \bar{h}_{fg}}{(\bar{T}_b - \bar{T}_a)\bar{h}_1}]; \quad \text{at } 0 < x < 1 \tag{15a}$$

$$\lambda = 0; \text{ at } x = 0 \tag{15b}$$

$$\frac{d\lambda}{dx} + Bi_2\lambda = 0; \quad \text{at } x = 1 \tag{15c}$$

where $F_7(x) = r^2(x)$, $F_8(x) = \pi r(x)$ and $F_9(x) = r(x)$ for spine fully wet fins and $F_7(x) = r(x)$, $F_8(x) = w$ and $F_9(x) = 1$ for longitudinal fully wet fins.

Finally, the following integral term is left for spine fully wet fins

$$\Delta J = \int_{x=0}^{1} \{2\pi[2(q-\Phi Q)(\theta-\Phi)+2\alpha r(v-V)]+[2r\lambda\frac{d\theta}{dx}\delta(x-1)-2r\frac{d\theta}{dx}\frac{d\lambda}{dx}] - 2\lambda Bi_1[\theta-\frac{\bar{h}_m\bar{h}_{fg}}{\bar{h}_1(\bar{T}_b-\bar{T}_a)}(\bar{\omega}-\bar{\omega}_a)\}\Delta r dx \tag{16a}$$

and the following integral term is left for longitudinal fully wet fins

$$\Delta J = \int_{x=0}^{1} \{2\alpha w(v-V)+[\lambda\frac{d\theta}{dx}\delta(x-1)-\frac{d\theta}{dx}\frac{d\lambda}{dx}]\}\Delta r dx \tag{16b}$$

Where $\delta(\bullet)$ is the Dirac delta function. From definition [Alifanov (1974)], the functional increment can be presented as

$$\Delta J = \int_{x=0}^{1} J'\Delta r dx \tag{16c}$$

A comparison of equations (16a), (16b) and (16c) leads to the following expression for the gradient J'(x) of the functional $J[r(x)]$ for spine and longitudinal fins, respectively:

$$J'(x) = 2\pi[2(q-\Phi Q)(\theta-\Phi)+2\alpha r(v-V)] + [2r\lambda\frac{d\theta}{dx}\delta(x-1)-2r\frac{d\theta}{dx}\frac{d\lambda}{dx}]-2\lambda Bi_1[\theta-\frac{\bar{h}_m\bar{h}_{fg}}{\bar{h}_1(\bar{T}_b-\bar{T}_a)}(\bar{\omega}-\bar{\omega}_a)], \text{ for spine fins} \tag{17a}$$

and

$$J'(x) = 2\alpha w(v-V)+\left[\lambda\frac{d\theta}{dx}\delta(x-1)-\frac{d\theta}{dx}\frac{d\lambda}{dx}\right], \quad \text{for longitudinal fins} \tag{17b}$$

The calculation of gradient equations is the most important part of CGM since it plays a significant role of the optimum fin calculation.

7 Computational Procedure

The computational procedure for the solution of this fully wet fin design problem using conjugate gradient method may be summarized as follows:

Suppose $r^n(x)$ is available at iteration n.

Step 1. Solve the direct problem given by equation (2) for θ(x).

Step 2. Examine the stopping criterion ε. Continue if not satisfied.

Step 3. Solve the adjoint problem given by equation (15) for λ(x).

Step 4. Compute the gradient of the functional J'^{n} from equation (17).

Step 5. Compute the conjugate coefficient γ^n and direction of descent P^n from equations (7c) and (7b), respectively.

Step 6. Set $\Delta r(x) = P^n(x)$, and solve the sensitivity problem given by equation (8) for $\Delta\theta(x)$. Then Δq, ΔQ and Δv can be calculated.

Step 7. Compute the search step size β^n from equation (12).

Step 8. Compute the new estimation for $r^{n+1}(x)$ from equation (7a) and return to step 1.

8 Results and Discussions

The purpose of this work is to apply the CGM in the present inverse fin design algorithm in estimating the optimum shapes for the fully wet longitudinal and spine fins based on the desired fin efficiency and fin volume.

Before examining the inverse design problem that we are going to consider here, one should make sure first that the solution for the direct problem is correct, otherwise the discussions of the optimum design solutions will become meaningless. For all the calculations considered in this work, the equations for determining the specific humidity $\bar{\omega}$ are adopted from Sharqawy and Zubair (2007).

To test the accuracy of the present numerical solution we have solved for the temperature distributions and fin efficiency for longitudinal and spine fins, respectively, and then compared with the results obtained from analytical expressions [Sharqawy and Zubair (2008, 2009)].

The following calculation conditions were considered in Sharqawy and Zubair (2008) for longitudinal fins and in Sharqawy and Zubair (2009) for spine fins:

$$m_0\bar{L} = \sqrt{\frac{2\bar{h}_1}{\bar{k}\bar{r}(0)}}\bar{L} = \sqrt{\frac{2Bi_1\bar{L}}{\bar{r}(0)}} = 0.8; \quad \bar{T}_a = 27^\circ\text{C}; \quad \bar{T}_b = 7^\circ\text{C} \tag{18}$$

Fin thickness at fin base can always be calculated for any specified fin volume

with given fin length, and therefore the Biot number Bi_1 can also be calculated in Equation (18) and used in Equation (2) for fin temperature calculations. When fin volume equals 0.003 and fin length equals 1, the Biot number for rectangular and concave longitudinal fin profiles are obtained as $Bi_1 = 0.00096$ and 0.00288, respectively. Similarly the Biot number for pin and concave spine fin profiles are obtained as $Bi_1 = 0.00989$ and 0.02211, respectively.

For the case when space increment used in finite difference equation of fin is taken as $\Delta x = 0.01$, and $Bi_2 = 0$, the exact [Sharqawy and Zubair (2008, 2009)] and numerical fin temperature distributions for fully wet longitudinal and spine fins using different fin profiles with relative humidity ϕ equal to 100%, 80%, 60% and 0% (dry fin) are shown in Figures 2 and 3, respectively. The exact [Sharqawy and Zubair (2008, 2009)] and numerical fin efficiency η for various fin profiles and working conditions are also shown in Tables 1a and 1b for longitudinal and spine fines, respectively. From these results it is concluded that the numerical solution for the direct problem is very accurate in the present study.

Table 1(a): The comparison of exact and numerical longitudinal fin efficiency.

Fin volume	Relative humidity	Bi_1	Rectangular fin		Triangular fin		Concave fin	
			Exact	Numerical	Exact	Numerical	Exact	Numerical
V	ϕ		η	η	η	η	η	η
0.015	60%	0.05	0.239	0.240	0.308	0.308	0.337	0.337
		0.075	0.195	0.196	0.256	0.256	0.286	0.286
		0.1	0.169	0.170	0.224	0.225	0.253	0.253
	80%	0.05	0.229	0.230	0.297	0.296	0.326	0.326
		0.075	0.187	0.188	0.247	0.247	0.276	0.276
		0.1	0.162	0.163	0.216	0.216	0.244	0.244
	100%	0.05	0.222	0.223	0.288	0.288	0.318	0.318
		0.075	0.181	0.182	0.240	0.240	0.269	0.269
		0.1	0.157	0.158	0.209	0.210	0.238	0.238

One should note that the initial guess of the fin shape is always necessary for the present iterative algorithm. To make it more convenient to be applied, it is always assumed that, for a fixed fin volume, the initial shapes for longitudinal and spine fin design problems are the rectangular and pin fins, respectively.

To illustrate the ability of the present inverse design algorithm in estimating the optimum shape for fins from the knowledge of the desired fin efficiency, the following two problems are considered, i.e. (I). the fully wet longitudinal fin design problems and (II). the fully wet spine fin design problems.

Table 1(b): The comparison of exact and numerical spine fin efficiency.

Fin volume	Relative humidity	Bi_1	Pin fin		Conical fin		Concave fin		Convex fin	
			Exact	Numerical	Exact	Numerical	Exact	Numerical	Exact	Numerical
V	ϕ		η	η	η	η	η	η	η	η
0.005	60%	0.5	0.123	0.123	0.286	0.286	0.421	0.421	0.208	0.208
		0.75	0.100	0.101	0.239	0.239	0.361	0.361	0.171	0.171
		1	0.087	0.087	0.210	0.210	0.322	0.322	0.149	0.149
	80%	0.5	0.118	0.118	0.276	0.276	0.408	0.408	0.199	0.199
		0.75	0.096	0.096	0.230	0.230	0.349	0.349	0.164	0.165
		1	0.083	0.083	0.202	0.202	0.311	0.311	0.143	0.143
	100%	0.5	0.114	0.114	0.268	0.268	0.399	0.399	0.194	0.194
		0.75	0.093	0.093	0.224	0.224	0.341	0.341	0.160	0.160
		1	0.081	0.081	0.196	0.196	0.303	0.304	0.139	0.139

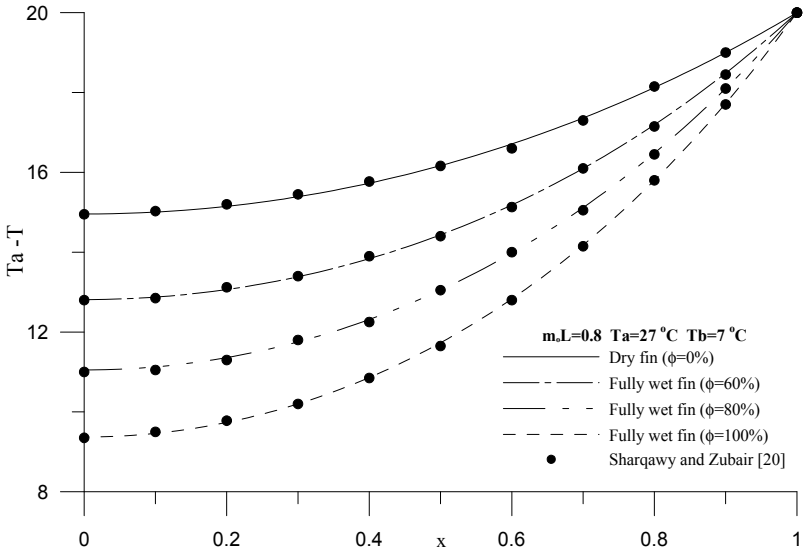

Figure 2(a): The comparison of present numerical solutions with exact solutions for rectangular longitudinal fin profile.

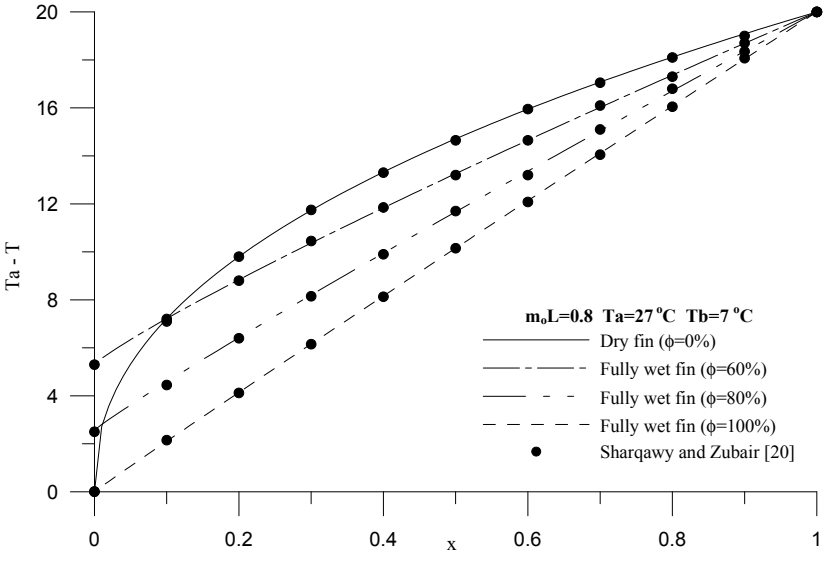

Figure 2(b): The comparison of present numerical solutions with exact solutions for concave longitudinal fin profile.

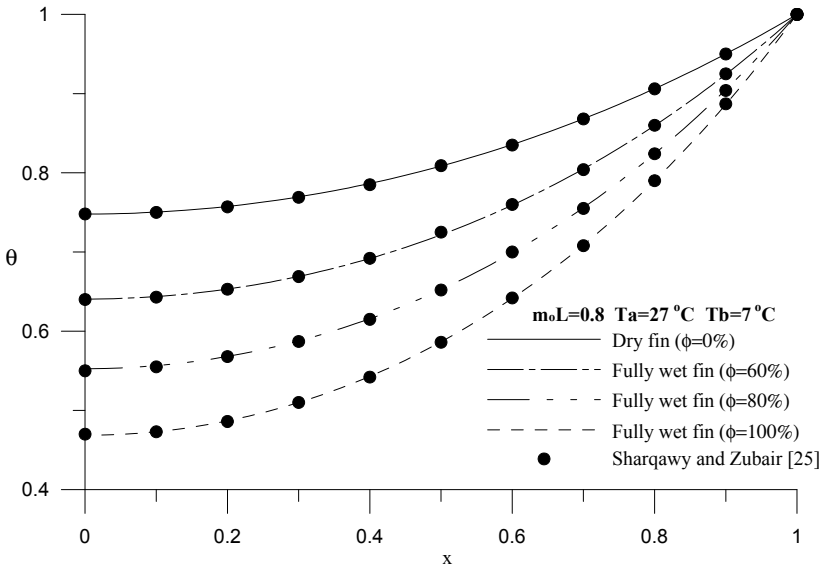

Figure 3(a): The comparison of present numerical solutions with exact solutions for pin spine fin profile.

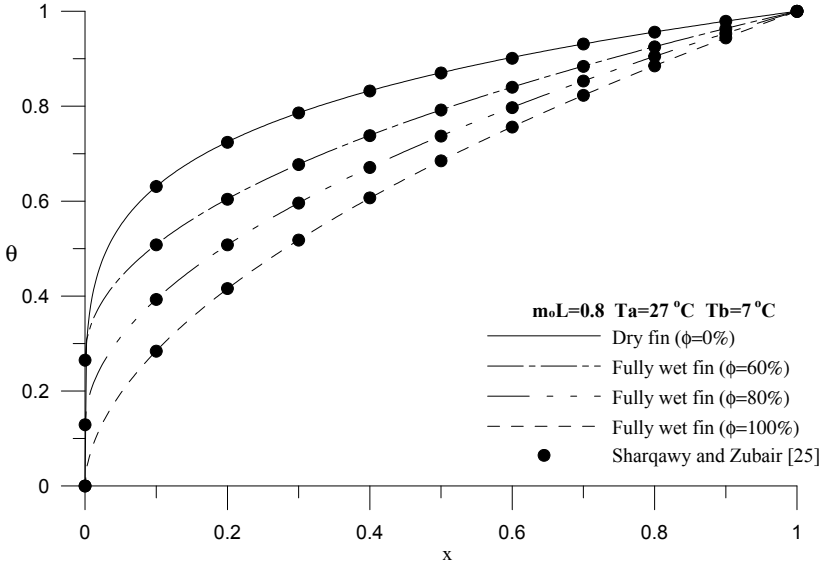

Figure 3(b): The comparison of present numerical solutions with exact solutions for concave spine fin profile

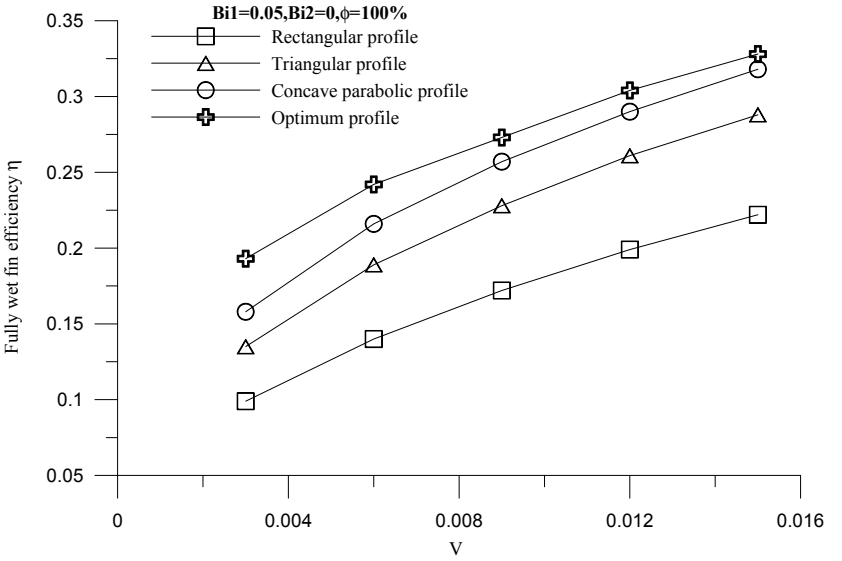

Figure 4(a): The comparison of fin efficiency for longitudinal fins with $Bi_1 = 0.05$ and $\phi = 100\%$.

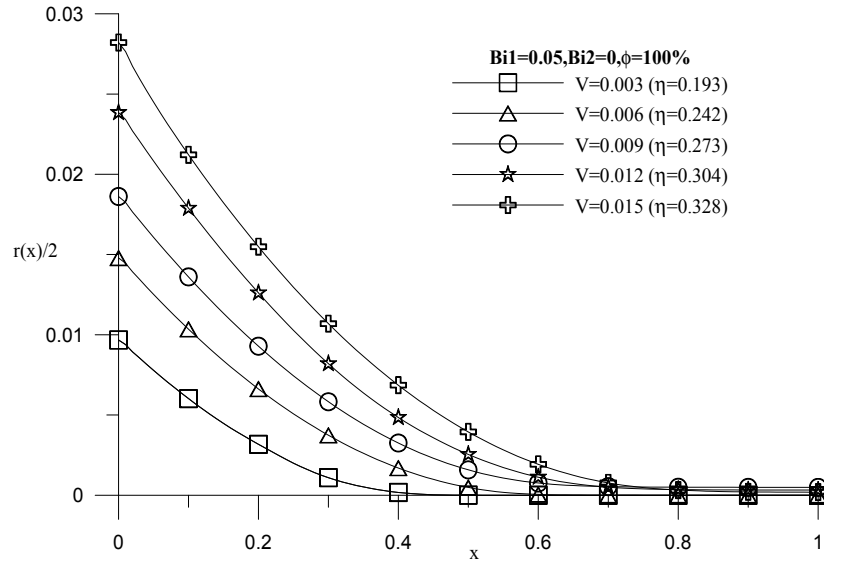

Figure 4(b): The optimum fin shapes for longitudinal fins with $Bi_1 = 0.05$ and $\phi = 100\%$

8.1 The Fully Wet Longitudinal Fin Design Problems

The optimum shape of longitudinal fins is first examined by considering perfect fin efficiency, i.e. $\Phi = 1.0$ and using $\Delta x = 0.01$, $Bi_1 = 0.05$, 0.075 and 0.1, $Bi_2 = 0$ and $\phi = 100\%$, 80% and 60%, respectively. The desired fin volume is given in the range from V = 0.003 to V = 0.015 with increment 0.003 and the width of fin w is assumed as unity. It is impossible to obtain the optimum shape of longitudinal fin having $\Phi = 1.0$, but the fin shape with best fin efficiency can still be obtained.

The determination of value for weighting coefficient α is important in the present algorithm since its value affects the rate of convergence. When α is small, the constraint for fin volume is loose which means the estimated fin volume may have discrepancy with the desired fin. At the same time, the product of β^n and P^n (i.e. the corrected value of fin radius) becomes larger, this also implies that the rate of convergent will be faster. To compromise with both requirements, the value of α is chosen as 10000 at the beginning and is increased gradually during the iterative process.

The value of objection function J can not be decreased to a small number for the case $\Phi = 1.0$, therefore the iterative process is stopped when $(J^n - J^{n-1}) < 10^{-8}$. By executing the above stated inverse design algorithm, the optimum shape of fully wet longitudinal fin for various desired fin volumes can be obtained. The results of these optimum fin design problems are also summarized in Table 2.

Figure 4a indicates the optimum efficiency of the estimated longitudinal fin and three commonly seen longitudinal fins with rectangular, triangular and concave parabolic profiles with $\phi = 100\%$. Figure 4b shows the estimated optimum fin shape for different given fin volumes with $\phi = 100\%$.

From Figures 4a, 4b and Table 2 we learned that for a fixed fin volume, the efficiency of the optimum fin is just slightly higher than the common longitudinal fins. This is because the fin width w is fixed and we can adjust only the fin thickness r(x) to optimize the fin efficiency. However, the fin thickness has much less weight than fin width in calculating the total fin surface. For this reason the optimum fin shape can improve only slightly the fin efficiency. Moreover it is noticed that the optimum fin efficiency increases as relative humidity ϕ decreases. This is because that when ϕ decreases the specific humidity $\bar{\omega}$ also decreases and this will increase the humidity difference between ambient air and fin surface, as a result increase the fin efficiency.

It is of interest to check the influence of Biot number Bi_1 on the estimated fin efficiency and fin shape. Figure 5a shows the optimum fin efficiency for different fin volumes when Bi_1 is increased from 0.05 to 0.075 and then to 0.1 with $Bi_2 = 0$ and $\phi = 60$ %. From this figure it is noticed that as the Biot number Bi_1 increases,

Table 2: The estimated results for longitudinal fin design problems.

Desired Efficiency	Desired Volume	Biot No.	Estimated Volume	Final Fin Efficiency			Number of Iterations		
Φ	V	Bi_1	V	$\phi = 100\%$	$\phi = 80\%$	$\phi = 60\%$	$\phi = 100\%$	$\phi = 80\%$	$\phi = 60\%$
1	0.003	0.05	0.003	0.193	0.198	0.203	80	92	367
	0.006		0.006	0.242	0.249	0.256	174	276	126
	0.009		0.009	0.273	0.284	0.294	980	492	272
	0.012		0.012	0.304	0.314	0.323	492	27	186
	0.015		0.015	0.328	0.337	0.348	13	60	216
	0.003	0.075	0.003	0.168	0.173	0.178	39	136	626
	0.006		0.006	0.211	0.218	0.224	45	49	109
	0.009		0.009	0.243	0.248	0.256	62	181	279
	0.012		0.012	0.267	0.273	0.277	330	386	353
	0.015		0.015	0.289	0.295	0.304	54	38	150
	0.003	0.1	0.003	0.153	0.157	0.161	91	300	304
	0.006		0.006	0.192	0.198	0.203	193	57	39
	0.009		0.009	0.221	0.226	0.233	33	77	167
	0.012		0.012	0.242	0.249	0.254	409	51	484
	0.015		0.015	0.262	0.268	0.277	113	45	253
0.2	0.006	0.05	0.006	0.199	0.199	0.200	16	12	73
	0.009		0.009	0.199	0.200	0.199	16	9	49
	0.012		0.012	0.199	0.199	0.200	5	6	31
	0.015		0.015	0.200	0.200	0.200	9	11	11
	0.006	0.075	0.006	0.199	0.199	0.199	18	15	15
	0.009		0.009	0.199	0.199	0.199	19	107	13
	0.012		0.012	0.199	0.200	0.200	27	77	85
	0.015		0.015	0.200	0.200	0.199	14	14	8
	0.009	0.1	0.009	0.199	0.199	0.199	15	16	19
	0.012		0.012	0.199	0.199	0.199	15	15	17
	0.015		0.015	0.199	0.199	0.199	18	13	15
0.25	0.009	0.05	0.009	0.249	0.250	0.249	19	14	13
	0.012		0.012	0.249	0.249	0.250	17	17	10
	0.015		0.015	0.249	0.249	0.249	23	13	13
	0.012	0.075	0.012	0.249	0.249	0.249	15	15	49
	0.015		0.015	0.249	0.249	0.250	13	13	39
	0.015	0.1	0.015	0.249	0.249	0.250	25	11	48

the optimum fin efficiency decreases. The reason for this is because when Bi_1 increases the fin surface temperature will become closer to ambient air temperature and this will decrease the temperature difference between them, as a result decrease the fin efficiency.

Figure 5b shows the optimum fin shapes for Bi_1 = 0.05, 0.075 and 0.1, respectively with fixed fin volume V = 0.009 and relative humidity ϕ= 60 %. Table 2 listed some information for the optimum longitudinal fully wet fin design problems that were considered here. From Figure 5b and Table 2, it is learned that as the Biot number increases, the fin base thickness r(0) also increases but the rest part of fin thickness r(x) decreases to obtain lower fin surface temperature and specific humidity and thus increase fin efficiency.

Next we will examine the present design algorithm by giving both designed fin

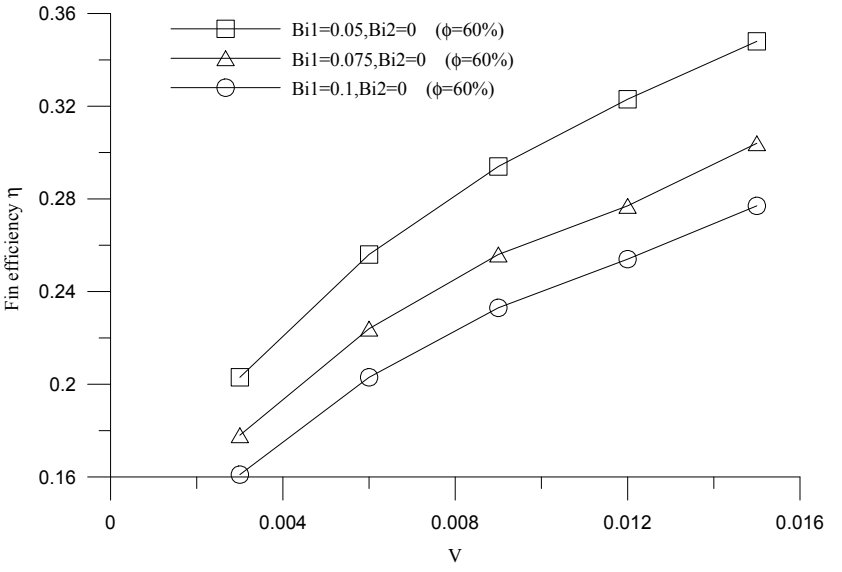

Figure 5(a): The optimum fin efficiency for longitudinal fins by varying Bi_1.

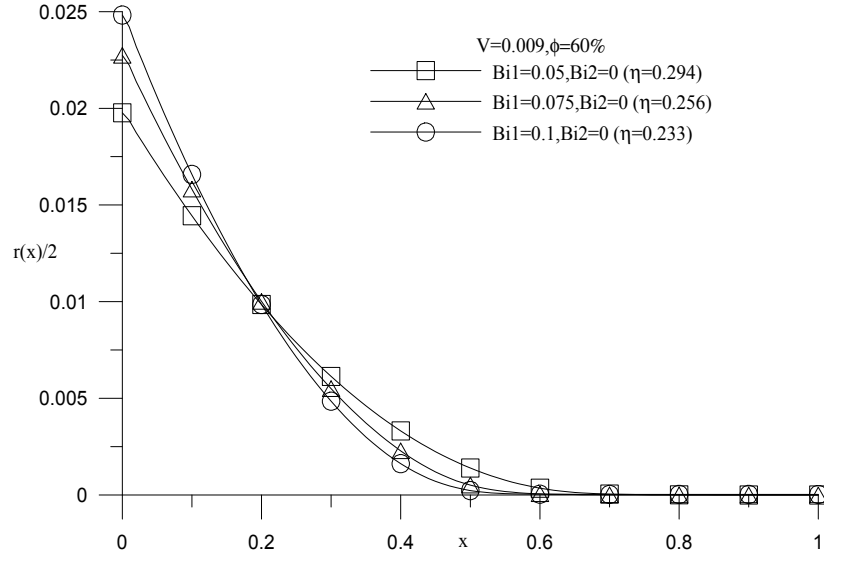

Figure 5(b): The optimum fin shapes for longitudinal fins at V = 0.009 by varying Bi_1.

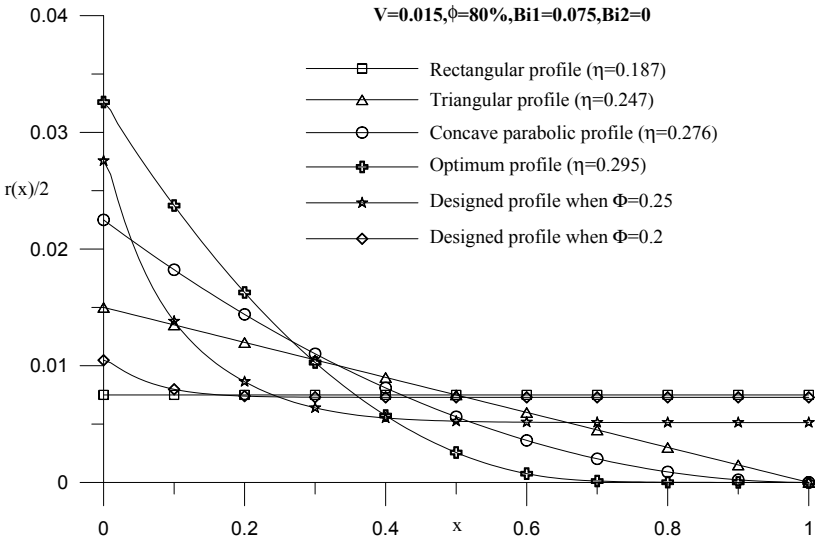

Figure 6(a): The designed fin shapes for longitudinal fins at $V = 0.015$, $\phi = 80\%$ and $Bi_1 = 0.075$.

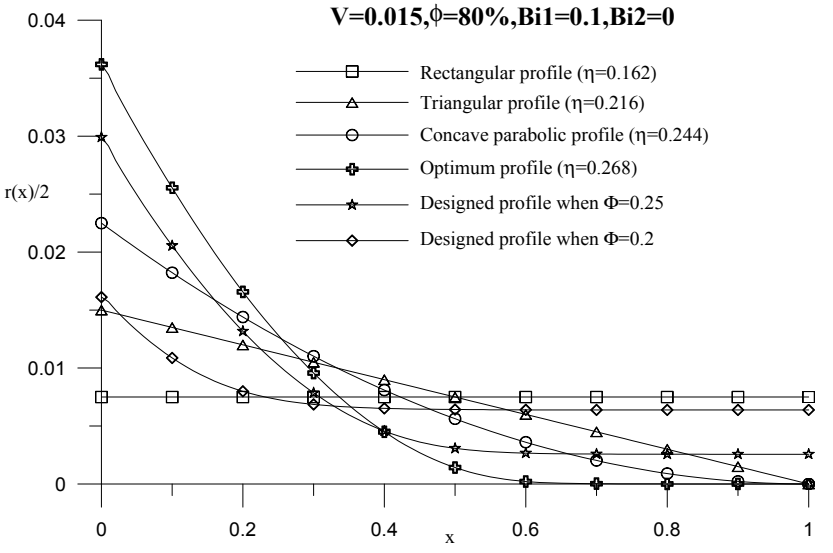

Figure 6(b): The designed fin shapes for longitudinal fins at $V = 0.015$, $\phi = 80\%$ and $Bi_1 = 0.1$.

efficiency and fin volume, then estimate the optimum fin shape that corresponding to different relative humidity. The desired fin efficiency is always less than the optimum efficiency, it is expected that the value of the objection function J can be decreased to a small number, so the stopping criteria under this consideration is taken as $\varepsilon = 10^{-8}$.

A comparison of optimum fin shape with the fin shapes with efficiency $\Phi = 0.2$ and 0.25 and three common longitudinal fins is shown in Figure 6a for $V = 0.015$, $Bi_1 = 0.075$, $Bi_2 = 0.0$ and $\phi = 80$ %. Then similar calculating conditions except for $Bi_1 = 0.1$ are used and the results are presented in Figure 6b. From Figures 6a and 6b it can be learned that as the desired fin efficiency is less than the optimum efficiency, fin base thickness $r(0)$ becomes thinner but the rest of fin thickness $r(x)$ becomes thicker. Moreover the outer edge of the fin surface will become thicker than the optimum one.

8.2 The Fully Wet Spine Fin Design Problems

Firstly, the optimum shape of fully wet spine fins is examined by considering perfect fin efficiency, i.e. $\Phi = 1.0$ and using $\phi = 60\%$, 80% and 100%, $\Delta x = 0.01$, $Bi_1 = 0.5$, 0.75 and 1.0, $Bi_2 = 0$. The desired fin volume is given in the range from V = 0.002 to V = 0.005 with increment 0.001. It is impossible to obtain the shape of spine fin having $\Phi = 1.0$ under this consideration, however, the optimum fin shape can still be obtained with best fin efficiency.

The value of α is chosen as 10000 at the beginning and is increased gradually during the iterative process as was mentioned previously. The stopping criteria under this consideration is that when$(J^n - J^{n-1}) < 10^{-10}$, stop the iterative process. By performing the above stated inverse design algorithm, the optimum shape of fully wet spine fin for various desired fin volumes can be obtained. The results of these optimum fin design problems are also summarized in Table 3.

From Table 3 it is noticed that as the Biot number Bi_1 increases, the optimum fin efficiency η also increases. For a fin with fin shape fixed, when Bi_1 is increased fin surface temperature will be decreased, as a result, the fin efficiency will also be decreased. However, in the present case, the fin shape can be adjusted automatically by the present algorithm to obtain optimum shape that matches best with the constraints. Therefore, it is possible that the fin efficiency increases even when Biot number increases.

Figure 7a shows the efficiency of the estimated optimum spine fin and four commonly seen spine fins with $Bi_1 = 1.0$, $\phi = 100\%$ and V = 0.002 to 0.005. Figure 7b illustrated the estimated optimum fin shape for various desired fin volumes. From Table 3, Figures 7a and 7b it is learned that for same desired fin volume, the effi-

Table 3: The estimated results for spine fin design problems.

Desired Efficiency	Desired Volume	Biot No.	Estimated Volume	Fin Efficiency			Number of Iterations		
Φ	V	Bi_1	V	$\phi = 100\%$	$\phi = 80\%$	$\phi = 60\%$	$\phi = 100\%$	$\phi = 80\%$	$\phi = 60\%$
1	0.002	0.5	0.002	0.908	0.904	0.896	144	99	98
	0.003		0.003	0.902	0.896	0.894	117	89	121
	0.004		0.004	0.897	0.895	0.884	191	84	111
	0.005		0.005	0.893	0.891	0.875	61	49	96
	0.002	0.75	0.002	0.913	0.908	0.899	61	112	108
	0.003		0.003	0.903	0.900	0.899	96	99	58
	0.004		0.004	0.901	0.904	0.888	87	46	20
	0.005		0.005	0.897	0.897	0.879	101	96	81
	0.002	1	0.002	0.916	0.912	0.902	133	61	143
	0.003		0.003	0.910	0.903	0.903	134	151	100
	0.004		0.004	0.904	0.908	0.892	149	35	107
	0.005		0.005	0.899	0.901	0.882	135	34	127
0.8	0.002	0.5	0.002	0.800	0.799	0.799	7	12	51
	0.003		0.003	0.800	0.800	0.799	10	52	10
	0.004		0.004	0.799	0.799	0.800	52	42	22
	0.005		0.005	0.800	0.800	0.799	45	11	32
	0.002	0.75	0.002	0.800	0.799	0.799	8	9	8
	0.003		0.003	0.799	0.799	0.800	10	8	51
	0.004		0.004	0.800	0.800	0.800	7	53	9
	0.005		0.005	0.800	0.799	0.799	9	48	28
	0.002	1	0.002	0.799	0.800	0.799	43	9	14
	0.003		0.003	0.800	0.799	0.800	8	15	8
	0.004		0.004	0.799	0.799	0.799	15	10	58
	0.005		0.005	0.799	0.799	0.799	12	54	32
0.6	0.002	0.5	0.002	0.600	0.600	0.599	12	10	25
	0.003		0.003	0.599	0.600	0.600	11	24	13
	0.004		0.004	0.599	0.599	0.599	25	14	40
	0.005		0.005	0.600	0.599	0.600	12	10	34
	0.002	0.75	0.002	0.600	0.600	0.600	12	12	8
	0.003		0.003	0.600	0.599	0.600	14	9	16
	0.004		0.004	0.600	0.599	0.599	9	23	12
	0.005		0.005	0.599	0.599	0.599	30	13	46
	0.002	1	0.002	0.600	0.600	0.599	8	9	23
	0.003		0.003	0.600	0.599	0.599	11	19	28
	0.004		0.004	0.600	0.599	0.599	9	29	36
	0.005		0.005	0.600	0.599	0.600	10	11	17

ciency of the optimum fin is indeed higher than that for the conventional spine fins.

Figures 8a and 8b show the optimum fin shapes for Bi_1 = 0.5, 0.75 and 1 with desired fin efficiency Φ = 0.8 and desired fin volume V = 0.003 at ϕ = 100% and 60%, respectively, with $\varepsilon = 10^{-10}$. From these two figures it is noted that as the Biot number and relative humidity increase, the fin base thickness $r(0)$ also increases but the rest part of fin thickness $r(x)$ decreases to obtain same fin efficiency and volume.

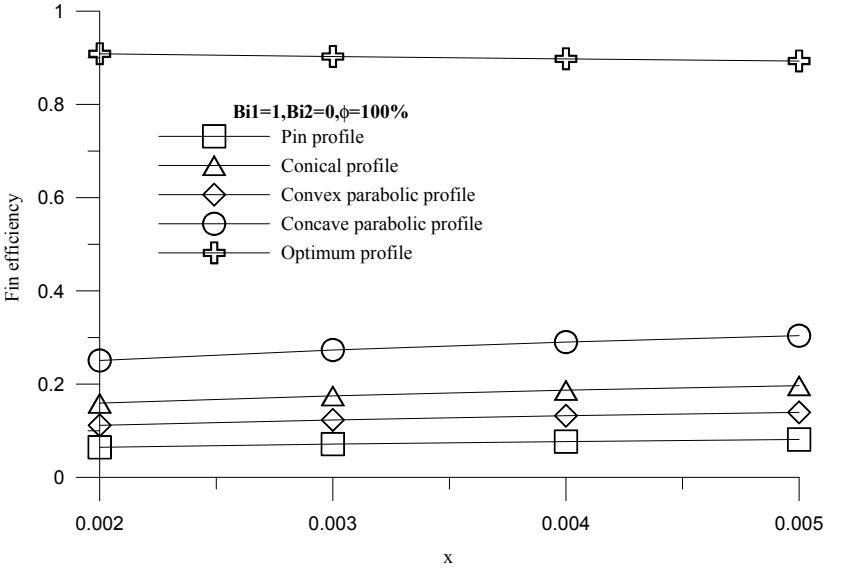

Figure 7(a): The comparison of fin efficiency for spine fins with $Bi_1 = 1.0$ and $\phi = 100\%$.

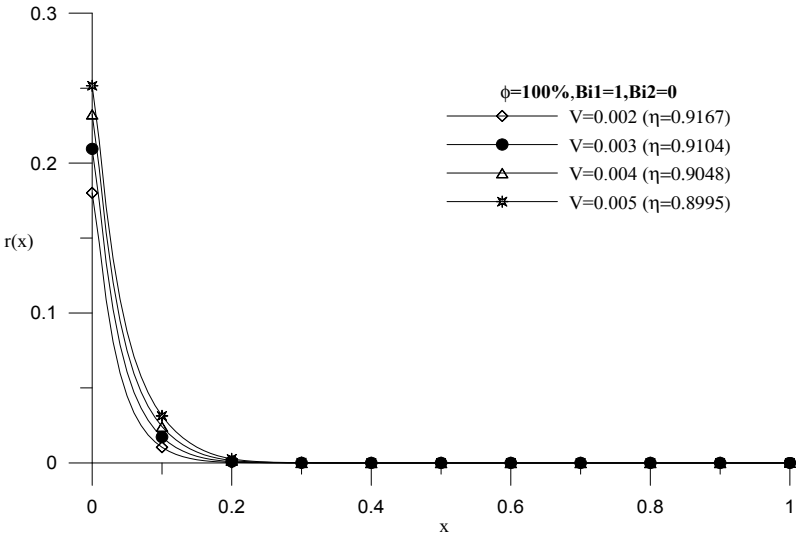

Figure 7(b): The optimum fin shapes for spine fins with $Bi_1 = 1.0$ and $\phi = 100\%$.

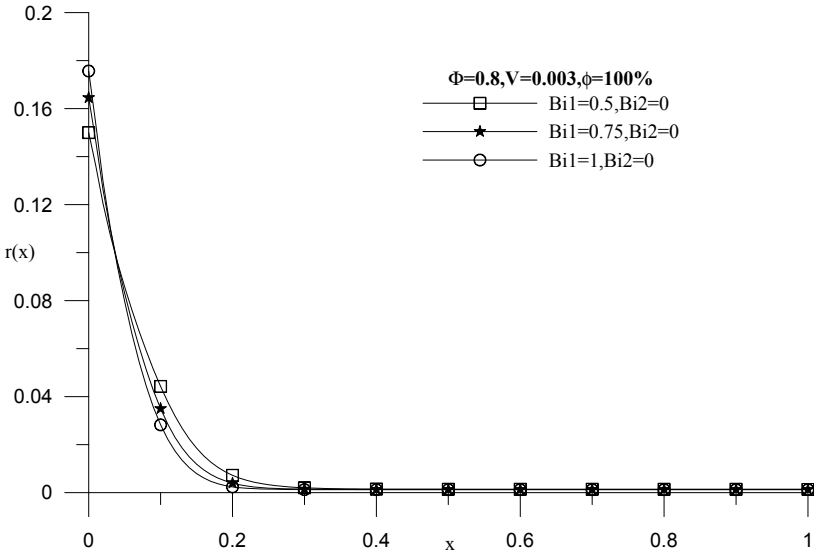

Figure 8(a): The designed spine fins at V = 0.003, ϕ = 100% and Φ = 0.8 by varying Bi_1.

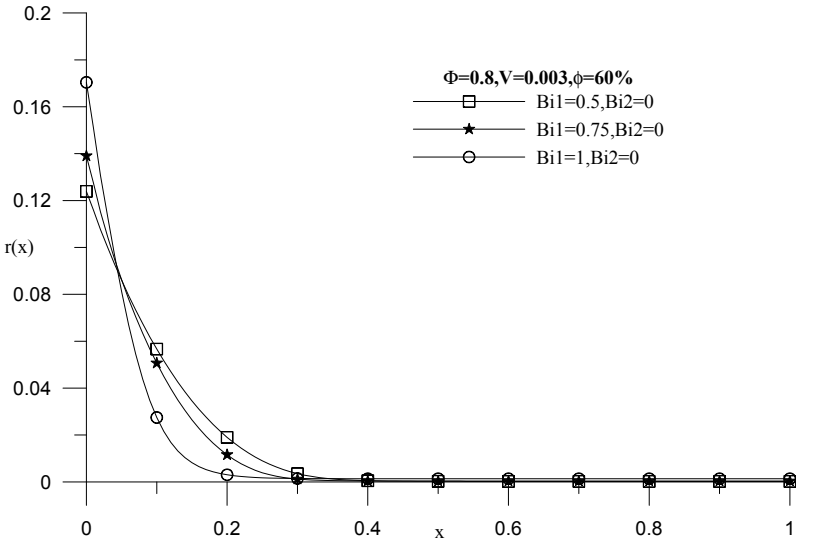

Figure 8(b): The designed spine fins at V = 0.003, ϕ = 60% and Φ = 0.8 by varying Bi_1.

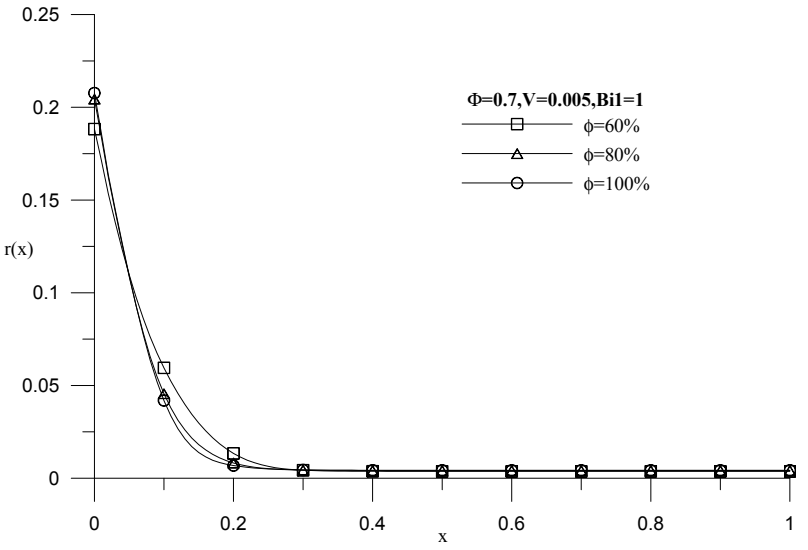

Figure 9(a): The designed spine fins at V = 0.005, Bi_1= 1.0 and Φ = 0.7 by varying ϕ.

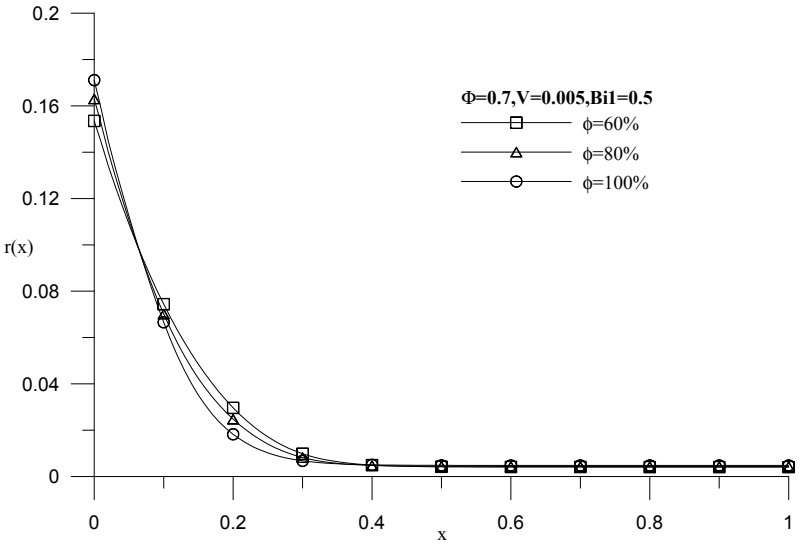

Figure 9(b): The designed spine fins at V = 0.005, Bi_1= 0.5 and Φ = 0.7 by varying ϕ.

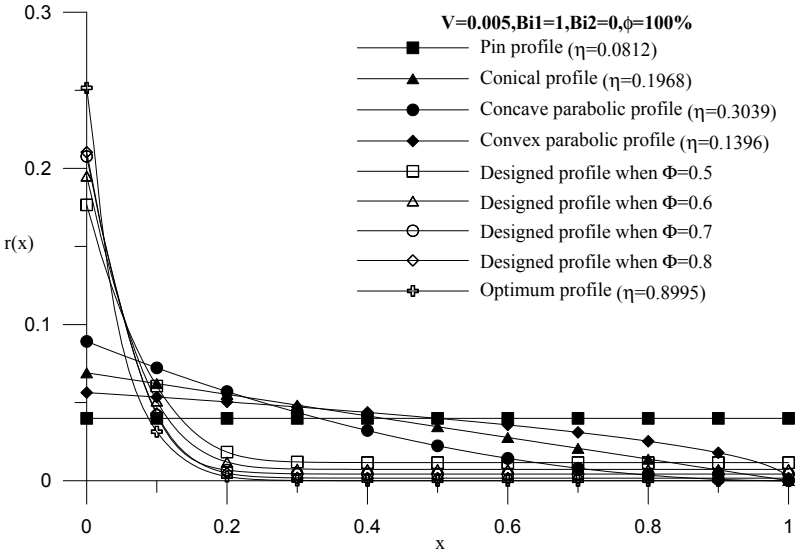

Figure 10(a): The comparison of optimum and designed fin shapes with many other fin shapes at V = 0.005 with Bi_1 = 1.0 and ϕ = 100%.

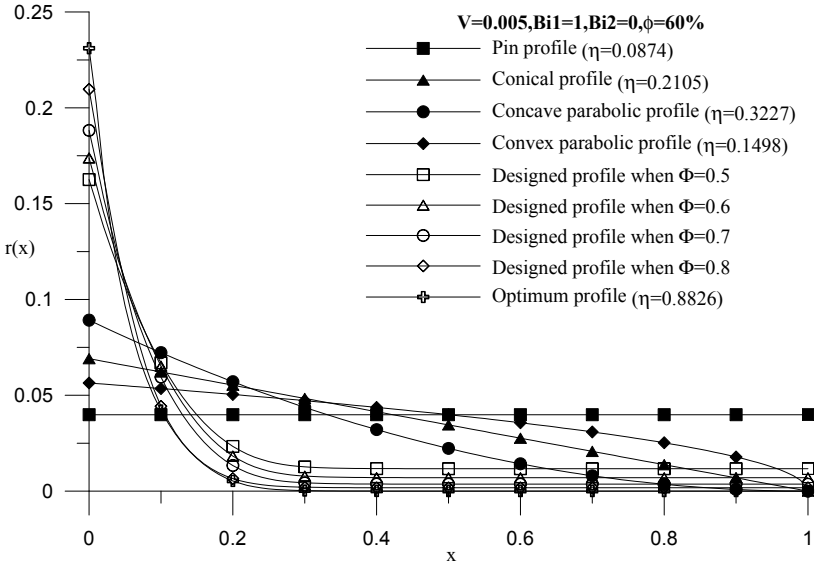

Figure 10(b): The comparison of optimum and designed fin shapes with many other fin shapes at V = 0.005 with Bi_1 = 1.0 and ϕ = 60%.

Figures 9a and 9b illustrate the optimum fin shapes for ϕ = 60%, 80% and 100% with desired fin efficiency $\Phi = 0.7$ and desired fin volume $V = 0.005$ at $Bi_1 = 1$, and 0.5, respectively. From Figures 9a and 9b we learned that the tendency is similar to that in Figures 8, i.e. as the Biot number and relative humidity increase, the fin base thickness $r(0)$ also increases.

Finally a comparison of optimum fin shape with the fin shapes of designed efficiency Φ = 0.5, 0.6, 0.7 and 0.8 and four commonly seen spine fins is shown in Figures 10a and 10b for V = 0.005, $Bi_1 = 1.0$ and $Bi_2 = 0.0$ at ϕ = 100 % and 60%, respectively. From Figures 10a and 10b it is learned that as the desired fin efficiency is less than the optimum efficiency, fin base thickness $r(0)$ becomes thinner but the rest of fin thickness $r(x)$ becomes thicker and the outer edge of the fin surface will become thicker than the optimum one to satisfy the desired fin volume.

From the above discussions it is concluded that the present fin design algorithm has the ability in designing optimum longitudinal and spine fully wet fins under the specified constraints and the rate of convergence is also very fast.

9 Conclusions

The conjugate gradient method (CGM) was applied successfully for the solution of the inverse design problem in estimating the optimum shape of the spine and longitudinal fully wet fins. Several test cases involving different design considerations were examined. The optimum fin shape obtained by the present design algorithm using the CGM always has higher fin efficiency than the commonly seen fins. Moreover, we also notice that when the Biot number and relative humidity are varied, the optimum fin efficiency and optimum fin shape will also be changed. The results also show that the fin efficiency can be improved greatly for the spine fully wet fins by the present design algorithm but can be increased only a little for the longitudinal fully wet fins.

Acknowledgement: This work was supported in part through the National Science Council, R. O. C., Grant number, NSC-97-2221-E-262-MY3.

References

Alifanov, O. M. (1974): Solution of an Inverse Problem of Heat Conduction by Iteration Methods. *J. of Engineering Physics*, 26: 471-476.

Aziz, A. (1992): Optimum Dimensions of Extended Surfaces Operating in a Convective Environment, *Applied Mechanics Review*, 45: 155-173.

Chung, B. T. F. (1983): Chapter 21 Heat Transfer, ASM Handbook for Engineering

Mathematics, American Society for Metals, Metal Park, OH.

Chung, B. T. F.; Iyer, J. R. (1993): Optimal Design of Longitudinal Rectangular Fins and Cylindrical Spines with Variable Heat Transfer Coefficient, *Heat Transfer Engng*, 14: 31-42.

Coney, J. E. R.; Sheppard, C. G. W.; El-Shafei, E. A. M. (1989): Fin Performance with Condensation from Humid Air: A Numerical Investigation, *International Journal of Heat and Fluid Flow*, 10: 224–231.

Duffin, R. J. (1959): A Variational Problem Related to Cooling Fins, *J. Math. Mech.*, 8: 47-56.

Huang, C.H.; Chen, C. A. (2008): The Shape Identification Problem in Estimating the Geometry of A Three-Dimensional Irregular Internal Cavity: *CMES: Computer Modeling in Engineering & Sciences*, 36:1-21.

Huang, C. H.; Hsiao, J. H. (2003): An Inverse Design Problem in Determining the Optimum Shape of Spine and Longitudinal Fins, *Numerical Heat Transfer, Part A*, 43: 155-177.

Huang, C. H.; Wu, H. H. (2007): A Fin Design Problem in Determining the Optimum Shape of Non-Fourier Spine and Longitudinal Fins. *CMC: Computers, Materials and Continua*, 5: 197–211.

Jeong, C.; Kallivokas, L. F. (2008): Inverse Scatterer Reconstruction in a Half-plane Using Surficial SH Line Sources. *CMES: Computer Modeling in Engineering & Sciences*, 35:49-71.

Kern, D. Q.; Kraus, A. D. (1972): Extended Surface Heat Transfer, MacGraw-Hill, New York.

Kraus, A. D. (1988): Sixty-five Years of Extended Surface Technology (1922-1987), *Applied Mechanics Review*, 41: 321-364.

Kundu, B. (2002): Analytical Study of the Effect of Dehumidification of Air on the Performance and Optimization of Straight Tapered Fins. *International Communications in Heat and Mass Transfer*, 29: 269–278.

Kundu, B. (2007): Performance and Optimization Analysis of SRC Profile Fins Subject to Simultaneous Heat and Mass Transfer, *International Journal of Heat and Mass Transfer*, 50: 1645–1658.

Kundu, B. (2008): Optimization of Fins Under Wet Conditions Using Variational Principle, *Journal of Thermophysics and Heat Transfer*, 22: 604–616.

Lasdon, L. S.; Mitter, S. K.; Warren, A. D. (1967): The Conjugate Gradient Method for Optimal Control Problem, *IEEE Transactions on Automatic Control*, AC-**12**: 132-138.

Liu, C. S. (2008): A lie-group shooting method for simultaneously estimating the time-dependent damping and stiffness coefficients. *CMES: Computer Modeling in Engineering & Sciences*, 27: 137-149.

McQuiston, F. C., (1975): Fin Efficiency with Combined Heat and Mass Transfer, *American Society of Heating, Refrigerating and Air-Conditioning Engineers Transactions*, 81: 350–355.

Mera, N. S. ; Elliott, L. ; Ingham, D. B. (2006) : The detection of super-elliptical inclusions in infrared computerized axial tomography. *CMES: Computer Modeling in Engineering & Sciences*, 15: 107-114.

Pirompugd, W.; Wang, C. C.; Wongwises, S. (2007): Heat and Mass Transfer Characteristics for Finned Tube Heat Exchangers with Humidification, *Journal of Thermophysics and Heat Transfer*, 21: 361–371.

Razelos, P. (1983): On Optimum Dimensions of Convective Pin Fins, *J. Heat Transfer*, 105: 411-413.

Sharqawy, M. H.; Zubair, S. M. (2008): Efficiency and Optimization of Straight Fins with Combined Heat and Mass Transfer – An Analytical Solution, *Applied Thermal Engineering*, 28: 2279–2288.

Sharqawy, M. H.; Zubair, S. M. (2007): Efficiency and Optimization of an Annular Fins with Combined Heat and Mass transfer – An Analytical Solution, International Journal of Refrigeration, 30: 751–757.

Sharqawy, M. H.; Zubair, S. M. (2009): Performance and Optimum Geometry of Spines with Simultaneous Heat and Mass Transfer, *International Journal of Thermal Sciences*, (Accepted, in press).

Schmidt, E. (1926): Die Warmeubertragung durch Rippen, Z. VDI, 70: 885-947.

Threlkeld, J. L. (1970): Thermal Environmental Engineering, second ed., Prentice-Hall, Inc, Englewood Cliffs, New Jersey.

Wilkins, Jr. J. E. (1960): Minimum Mass Thin Fins with Transfer Heat only by Radiation to Surrounding at Absolute Zero, *J. Soc, Ind, Appl, Math.*, 8: 630-639.

Wu, G.; Bong, T. Y. (1994): Overall Efficiency of a Straight Fin with Combined Heat and Mass Transfer, *American Society of Heating, Refrigerating and Air-Conditioning Engineers Transactions*, 100: 367–374.

Yeh, R. H. (1996): Optimum Dimensions of Longitudinal Rectangular Fins and Cylindrical Pin Fins with Variable Heat Transfer Coefficient, *The Canadian J. of Chemical Engineering*, 74: 144-151.